Abnormal Sperm in Mice Lacking the *Taf7l* Gene[▽][†]

Yong Cheng,[1] Mariano G. Buffone,[2] Martin Kouadio,[3] Mary Goodheart,[4] David C. Page,[4]
George L. Gerton,[2] Irwin Davidson,[3] and Peijing Jeremy Wang[1]*

*Department of Animal Biology, School of Veterinary Medicine, University of Pennsylvania, Philadelphia, Pennsylvania 19104[1];
Center for Research on Reproduction and Women's Health, Department of Obstetrics and Gynecology, University of
Pennsylvania Medical Center, Philadelphia, Pennsylvania 19104[2]; Institut de Génétique et de Biologie Moléculaire et
Cellulaire, CNRS/INSERM/ULP, 1 Rue Laurent Fries, 67404 Illkirch Cédex, France[3]; and
Howard Hughes Medical Institute, Whitehead Institute, and Department of Biology,
Massachusetts Institute of Technology, 9 Cambridge Center,
Cambridge, Massachusetts 02142[4]*

TFIID is a general transcription factor required for transcription of most protein-coding genes by RNA polymerase II. TAF7L is an X-linked germ cell-specific paralogue of TAF7, which is a generally expressed component of TFIID. Here, we report the generation of *Taf7l* mutant mice by homologous recombination in embryonic stem cells by using the Cre-*loxP* strategy. While spermatogenesis was completed in *Taf7l*$^{-/Y}$ mice, the weight of *Taf7l*$^{-/Y}$ testis decreased and the amount of sperm in the epididymides was sharply reduced. Mutant epididymal sperm exhibited abnormal morphology, including folded tails. Sperm motility was significantly reduced, and *Taf7l*$^{-/Y}$ males were fertile with reduced litter size. Microarray profiling revealed that the abundance of six gene transcripts (including *Fscn1*) in *Taf7l*$^{-/Y}$ testes decreased more than twofold. In particular, FSCN1 is an F-action-bundling protein and thus may be critical for normal sperm morphology and sperm motility. Although deficiency of *Taf7l* may be compensated in part by *Taf7*, *Taf7l* has apparently evolved new specialized functions in the gene-selective transcription in male germ cell differentiation. Our mouse studies suggest that mutations in the human *TAF7L* gene might be implicated in X-linked oligozoospermia in men.

TFIID, a general transcription factor, plays a central role in transcription initiation of most protein-coding genes by RNA polymerase II. TFIID is a multiprotein complex consisting of TATA-binding protein (TBP) and 12 to 15 TBP-associated factors (TAFs) (20, 35). The assembly of TFIID at the promoter region recruits other basal transcription factors and RNA polymerase II (2, 31). TAFs play important roles in transcriptional regulation. Some TAFs directly interact with transcriptional activators and thus serve as coactivators. In addition, interactions between TAFs are critical for promoter recognition and selectivity by RNA polymerase II (17, 36).

Strikingly, studies of a number of tissue-specific TAFs in *Drosophila melanogaster* and mouse have identified cell-type-specific transcription programs. In *Drosophila melanogaster*, five testis-specific homologues of widely expressed TAFs have been reported: Can (homologue of dTAF5), Nht (homologue of dTAF4), Mia (homologue of dTAF6), Sa (homologue of dTAF8), and Rye (homologue of dTAF12) (18, 19). Null mutations in *can*, *nht*, *mia*, and *sa* result in the same male sterile phenotype, and all four genes are required for meiotic cell cycle progression and onset of spermatid differentiation (27). In addition, Rye interacts with Nht, suggesting that these five testis-specific TAFs in *Drosophila* function in the same transcription regulatory pathway (18). Mechanistically, these TAFs may counteract transcriptional repression by Polycomb group (PcG) proteins in spermatocytes (8). In mice, TAF4B (homologue of TAF4) is highly expressed in the testis and the granulosa cells of the ovary, where it is required for follicular development (14). Testes of TAF4B-deficient males are initially normal but undergo progressive germ cell loss, resulting in male sterility by 3 months of age (12). In addition to tissue-restricted TAFs, TRF2 is a testis-specific homologue of TBP and is essential for spermiogenesis in mouse (28, 44). These results, together with other studies, support the presence of tissue-specific transcription programs in regulating germ cell differentiation (23, 33).

We have identified a testis-specific homologue of the generally expressed TAF7 in mouse, named TAF7L (30, 39). TAF7 interacts with multiple transcription activators (9). TAF7 also interacts with other TAFs, including TAF1 (the largest subunit of TFIID), but not with TAF10 or TBP (9, 24). Binding of TAF7 to TAF1 inhibits the acetyltransferase activity of TAF1, which is important for the transcription of major histocompatibility complex class I genes (16). Like TAF7 in somatic tissues, TAF7L interacts with TAF1 and is associated with TBP in testes, indicating that TAF7L is a bona fide TAF (30). Subcellular localization of TAF7L in male germ cells is dynamic. TAF7L is cytoplasmic in spermatogonia and early spermatocytes (preleptotene, leptotene, and zygotene); however, TAF7L translocates into the nuclei of pachytene spermatocytes and round spermatids. In contrast, TAF7 is nuclear from spermatogonia to pachytene spermatocytes and appears

---

to be absent in round spermatids. Biochemical studies indicate that TAF7L might replace TAF7 in the TFIID complex to modulate the transcription program in spermatogenesis (30). To assess the role of TAF7L in spermatogenesis, we generated mice lacking TAF7L by gene targeting in embryonic stem (ES) cells. Here, we describe the effects of this mutation on gene transcription and production, morphology, and motility of spermatozoa.

MATERIALS AND METHODS

Disruption of the *Taf7l* gene. In the *Taf7l* targeting construct, we introduced *loxP* sites into the first and sixth introns (see Fig. 2A). Using a *Taf7l*-containing bacterial artificial chromosome clone (RP22-415C9) as template, three DNA fragments (2 kb, 3.4 kb, and 3 kb) were amplified by high-fidelity PCR. The CMV-HyTK double-selection cassette is flanked by *loxP* sites and enables hygromycin-positive selection and thymidine kinase-negative selection. Three *loxP* sites in the final targeting construct are in the same orientation (see Fig. 2A). The construct was sequenced, except for the HyTK cassette, and no mutations were found.

Hybrid V6.5 ES cells (C57BL/6 × 129) were used for gene targeting (11). ES cells were electroporated with the linearized *Taf7l* targeting construct and selected for integration in the presence of hygromycin B (120 μg/ml; Invitrogen). Subsequently, 384 hygromycin-resistant ES cell colonies were screened for homologous recombination by PCR. Of the hygromycin-resistant clones, 9.4% contained the *Taf7l³ˡᵒˣ* allele. Twelve clones were subjected to Southern blot analysis and confirmed (data not shown).

Two *Taf7l³ˡᵒˣ*-positive ES cell clones were then electroporated with the pOG231 plasmid that transiently expresses Cre recombinase. Two days after electroporation, cells were passaged and then subjected to selection with ganciclovir (2 μM; Sigma) for removal of the HyTK cassette. Viable colonies were picked and screened by PCR. Recombination between the HyTK-flanking *loxP* sites resulted in the *Taf7lᶠˡᵒˣ* allele at a frequency of 12.5% (see Fig. 2A).

Generation and genotyping of mice. ES cells harboring the *Taf7lᶠˡᵒˣ* allele were injected into BALB/c blastocysts that were subsequently transferred to uteri of pseudopregnant Swiss Webster females. The resulting male chimeras were bred with BALB/c females to obtain germ line transmission of injected ES cells. Agouti females were genotyped by PCR. *Taf7lᶠˡᵒˣ* mice were crossed with ACTB-Cre transgenic mice to obtain the *Taf7l⁻* (mutant) allele (26). The ACTB-Cre transgene was subsequently removed from *Taf7l* mutant mice by breeding. We backcrossed *Taf7l⁺/⁻* mice to C57BL/6J (B6) and 129 strains for more than five generations (strain 129X1/SvJ, stock no. 000691; The Jackson Laboratory). Mice from either B6 or 129 backgrounds were used in this study. All offspring were genotyped by PCR. Wild-type (300-bp) and flox (490-bp) alleles were assayed by PCR with the primers CCATTCTTCTAAATCCCTAGC and TCGCTTGGGGAACTCATCAATT. The PCR product (218 bp) of the mutant allele was amplified by PCR with the primers CCATTCTTCTAAATCCCTAGC and CATCGTGTAATTTGGGGTTGAC.

Coimmunoprecipitation and Western blot analysis. Nuclear extracts from testes were prepared as previously described (30). Extracted proteins (10 μg) were separated by sodium dodecyl sulfate-polyacrylamide gel electrophoresis, and the presence of TBP, TAF7, and TAF7L was revealed using monoclonal antibodies 3G3, 19TA, and 46TA as previously described (6, 30). The filters were then reprobed with antibodies against TAF5 and TAF6 (4, 10). Immunoprecipitations were performed as previously described (30). Briefly, 200 μg of extract was immunoprecipitated with anti-TBP antibody (3G3) overnight at 4°C with 100 μl of protein G-Sepharose. Beads were washed three times for 10 min at room temperature with buffer A (20% glycerol, 50 mM Tris-HCl, pH 7.9, 1 mM EDTA, 1 mM dithiothreitol, 0.1% NP-40) containing 0.5 M KCl and once with buffer A containing 0.1 M KCl. Precipitated material was eluted using a peptide against the 3G3 epitope as described previously (6). Eluted proteins were probed on immunoblots using the antibodies described above.

EM and histology. Electron microscopy (EM) was performed at the Biomedical Imaging Core Facility at the University of Pennsylvania as previously described (42). Cauda epididymides from 8-week-old wild-type and *Taf7l⁻/Y* mice were fixed and processed for EM. For histological analysis, testes were fixed in Bouin's solution, embedded in paraffin, sectioned, and stained with hematoxylin and eosin as described previously (32).

Sperm count. Cauda epididymides were dissected and minced in phosphate-buffered saline solution. Sperm were squeezed out with fine forceps and allowed to disperse in phosphate-buffered saline at room temperature for 10 min, followed

by repeated pipetting. Samples were fixed in 4% paraformaldehyde. Sperm were counted using a hematocytometer. Sperm counting was performed four times for each sample.

Sperm motility assay. Uncapacitated cauda epididymal sperm from wild-type and *Taf7l⁻/Y* mice were collected by placing minced cauda epididymides in Krebs-Ringer bicarbonate medium (HM) without Ca^{2+}, bovine serum albumin, and $NaHCO_3$ as previously described (25). The working "complete" medium was prepared by adding $CaCl_2$ (1.7 mM), pyruvate (1 mM), $NaHCO_3$ (25 mM), and bovine serum albumin (3 mg/ml), followed by gassing with 5% CO_2 and 95% O_2 to pH 7.3. One drop of the sperm suspension was transferred to the incubation chamber at 37°C. The incubation time for capacitation was 1 hour at 37°C in a 5% CO_2-95% O_2 incubator. Aliquots of each sperm suspension were loaded into a 100-μm-deep chamber prewarmed at 37°C (Conception Technologies). Sperm motility parameters were quantified using a computer-assisted semen analysis system running IVOS (version 12.2L; Hamilton Thorne Research). At least 400 sperm per sample were analyzed. For statistical analysis, eight motion parameters, motility, average path velocity (VAP), straight-line velocity (VSL), curvilinear velocity (VCL), amplitude of lateral head displacement, beat-cross frequency (BCF), straightness, and linearity, were examined (see Table 2). For statistical testing, sperm motility measurements of each parameter were pooled for each genotype and for time of observation. Considering the log-normal distribution, Student's t test for independent observations was applied to define differences between the wild type and the mutant in VAP, VSL, VCL, and BCF means (normalized by natural logarithms). For the same purpose, the nonparametric amplitude of lateral head displacement and STR distributions were tested by Friedman's analysis of variance. Statistical analyses were performed using the InStat program (GraphPad software).

Microarray analysis. Total RNA was prepared from 8-week-old testes by using TRIzol reagent (Invitrogen) and subsequently purified using an RNeasy minikit (QIAGEN). Both wild-type and *Taf7l⁻/Y* testes were analyzed in duplicate. Five micrograms of total RNA from each sample was used for the generation of biotinylated cRNA. The cRNA samples were hybridized to Mouse Genome 430 2.0 GeneChips (Affymetrix) at the University of Pennsylvania Microarray Core Facility according to the manufacturer's expression analysis technical manual (Affymetrix). Microarray Analysis Suite 5.0 (Affymetrix) was used to quantify microarray signals. The Microarray Analysis Suite 5.0 metrics output was imported into GeneSpring v7 (Agilent Technologies) with normalization to the median of the Affymetrix spike-in controls. SAM (Statistical Analysis of Microarrays) two-paired analysis was applied to identify genes with significant differences at a 13% false discovery rate.

Quantitative and semiquantitative reverse transcription (RT)-PCR analyses. Total RNA was isolated from 8-week-old wild-type and *Taf7l⁻/Y* testes by using TRIzol reagent. One microgram of total RNA for each sample was converted into cDNA by reverse transcription with oligo(dT)₁₈V primers and was diluted to a final volume of 200 μl, 5 μl of which was used in each PCR. Three replicates were used for each real-time PCR. Reverse transcriptase-negative templates served as controls. Real-time PCR was run on a LightCycler (Roche). Quantification was normalized to *Actb* within the log phase of the amplification curve.

Spermatogenic cell populations enriched for specific germ cell types were the same as previously used, and their preparations have been described previously (41). Each enriched population contained a small amount of developmentally adjacent germ cells. A semiquantitative RT-PCR technique was used as previously described (41). Briefly, 70 ng of poly(A)⁺ RNA was used for reverse transcription primed with oligo(dT)₁₈V in a 25-μl reaction mixture. Each RT reaction was diluted to a total volume of 200 μl, and 5 μl was used for each PCR. To avoid saturation of PCR, products were taken after various cycles (20–30) and analyzed by gel electrophoresis. One microgram of total RNA from adult wild-type and XXᵞ* testes was used for reverse transcription. Controls without reverse transcriptase were negative (data not shown). The following gene-specific primers were used: *Actb*, AGAAGAGCTATGAGCTGCCT and TCATCGTACTCCTGCTTGCT; *Fscn1*, ACCGATCAGGAGACCTTCCA and GAGTCTTTGATGTTGTAGGCG; *4732473B16Rik*, TGAGCTGGCCACAGGTGAA and ACTTTGACCAGCTTCTGCAC; *Cpa6*, GAACCAGAAGTGAAGGCTGT and CTTTAGCAGGTGCATTGTGAT; *Adc*, GGGGTCTTCAACTCAGTCCT and ACAAGGTGTCTGTGATCTCC; *D1Ertd622e*, AACTTGCACAGTGACATCATC and AGTCCCGTGTCCAGCTGTTT; and *Sfmbt2*, GACGGATGTGGTACGATTCA and GTGCTCCTTCCGTGTGCTTT. Primers for *Pgk2* and *Prm1* have been described previously (43).

Microarray data accession number. Microarray tabular data have been deposited in the Gene Expression Omnibus database under accession no. GSE5510.
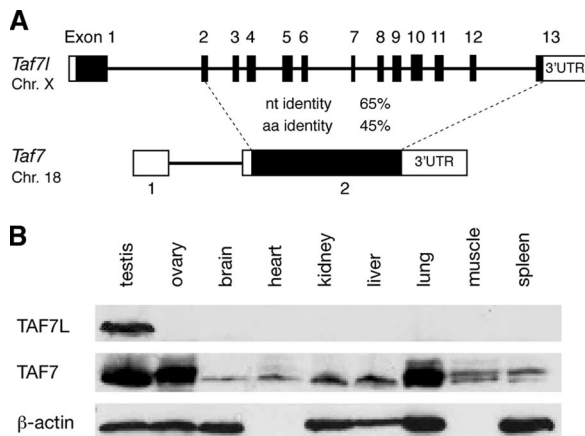
FIG. 1. Contrasting exon/intron structures and expression patterns of the mouse *Taf7l* and *Taf7* genes. (A) *Taf7* is a retroposed derivative of *Taf7l*. The gene structures were determined by alignment of *Taf7l* (accession no. AK017109) and *Taf7* (NM_011901) cDNA sequences with their genomic sequences. Coding regions are shown in black. Percent identities in the coding regions for nucleotide (nt) and aa sequences are indicated. Compared with TAF7, TAF7L contains ~100 additional residues at its amino terminus. No significant nt identity is present in the untranslated regions (UTR). (B) Western blot of TAF7L and TAF7 in adult mouse tissues. Equal amounts (20 μg) of protein extracts for each tissue were loaded. β-Actin served as a control. Chr., chromosome.

RESULTS

***Taf7l* is the ancestral gene of *Taf7* and has evolved to be testis specific.** While the *Taf7l* coding region is interrupted by 12 introns, the *Taf7* coding region completely lacks introns (Fig. 1A). This suggests that *Taf7l* is the ancestral gene and that *Taf7* is a retroposed paralogue of *Taf7l*. Interestingly, the *Slc25a2* gene, adjacent to *Taf7*, is also a retroposed gene (of *Slc25a*) (7). These two functional retroposed genes are located between the protocadherin alpha and beta gene clusters on mouse chromosome 18 and human chromosome 5. Thus, the *Taf7-Slc25a2* retroposition occurred prior to the radiation of eutherians (at least 80 million years ago). One intron is present in the 5′ untranslated region of the mouse *Taf7* gene (Fig. 1A). However, the *Taf7* orthologue in human and rat does not appear to have an intron. The most parsimonious explanation is that the acquisition of the single intron by *Taf7* is specific to the mouse lineage.

We then examined the expression of *Taf7* and *Taf7l* by Western blot analysis. While the TAF7 protein was present in all tissues examined at various abundances, TAF7L was testis specific (Fig. 1B). These data are in agreement with those of previous studies (30, 39, 45). There exist a number of precedents in which widely expressed intron-bearing ancestral genes gave rise to tissue-specific retroposed genes, particularly testis-specific genes (38). However, it is highly unusual for an ancestral gene such as *Taf7l*, initially widely expressed, to evolve tissue specificity.

Inactivation of the *Taf7l* gene. To elucidate the role of *Taf7l* in spermatogenesis, we generated a floxed *Taf7l* conditional allele (*Taf7l*[flox]) in mice (Fig. 2A). *Taf7l*[flox/Y] males and *Taf7l*[flox/flox] females displayed normal fertility. By crossing with ACTB-Cre transgenic mice, we obtained *Taf7l*[−/Y] mice that lack exons 2 to
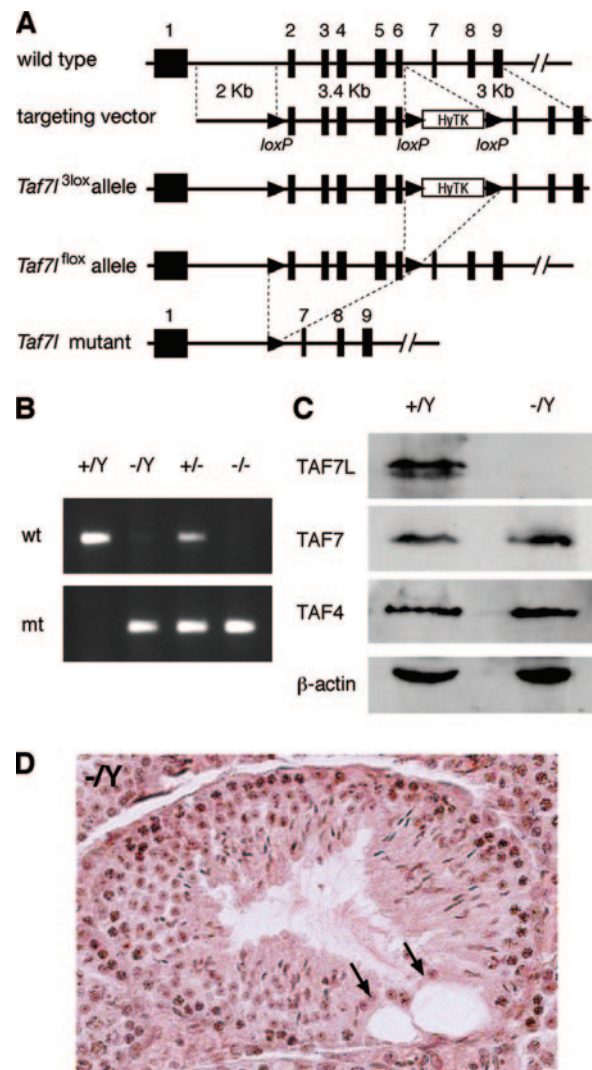

FIG. 2. Targeted inactivation of *Taf7l* in mice. (A) Schematic presentation of the *Taf7l* gene, the targeting construct, and various alleles. Exons 1 to 9 are shown as rectangles. Exons 10 to 13 are not shown. Deletion of exons 2 to 6 (aa 96 to 263) in the *Taf7l* mutant allele is expected to cause a frameshift. (B) Genotyping of *Taf7l* alleles. Genotypes are indicated. wt, wild-type allele; mt, *Taf7l* mutant allele. (C) Western blot of *Taf7l*[−/Y] testes. Equal amounts (20 μg) of testis protein extracts were loaded. TAF7L was absent in *Taf7l*[−/Y] testes. The abundances of TAF7 and TAF4 did not differ in *Taf7l*[−/Y] and wild-type testes. (D) Histological analysis of 7-month-old *Taf7l*[−/Y] testes. Two large vacuoles (arrows) were present in the seminiferous tubule, despite the presence of a full spectrum of germ cells.

6 (26). Deletion of exons 2 to 6 (amino acids [aa] 96 to 263) resulted in a frameshift. In ACTB-Cre mice, Cre recombinase is under the control of the human β-actin promoter and is widely expressed. In the hybrid genetic backgrounds, both *Taf7l*[−/Y] males and *Taf7l*^{−/−} females were fertile and the litter sizes were similar to that of wild-type controls. We backcrossed this knockout allele to C57BL/6 and 129 backgrounds (at least five backcrosses). All subsequent analyses were performed on both C57BL/6 and 129 mice, and no difference was observed. Western blot analysis showed that the TAF7L protein is absent
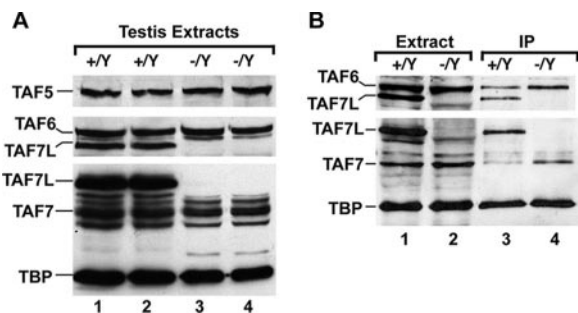
FIG. 3. Competition between TAF7 and TAF7L for association with TBP. (A) Expression analysis of TBP and TBP-associated factors in *Taf7l*$^{-/Y}$ testes. Ten micrograms of two independent extracts from testes of wild-type (*Taf7l*$^{+/Y}$) or *Taf7l*$^{-/Y}$ animals was probed with antibodies against the indicated proteins. The filter was then reprobed with antibodies against TAF5 and TAF6. (B) Results of coimmuno-precipitation assays. Lanes 1 and 2 show starting extracts from wild-type and mutant testes used for immunoprecipitation (IP) with anti-TBP antibody. Lanes 3 and 4 show peptide-eluted material from immunoprecipitations. The filter was probed with antibodies against TBP, TAF7, and TAF7L and then reprobed with antibodies against TAF6. To avoid masking TAF7 with a signal from the heavy chain of anti-TBP antibody used in immunoprecipitation, the blot was revealed using conjugated goat anti-mouse κ chain antibody as previously described (24).

TABLE 1. Sperm production in *Taf7l*$^{+/Y}$ and *Taf7l*$^{-/Y}$ mice[a]

Parameter	Value for genotype (mean ± SD)[b]		Ratio of −/Y value to +/Y value	P value
	+/Y	−/Y		
Body wt (g)	25.2 ± 2.6	25.8 ± 2.3	1.02	<0.55
Testicular wt (mg)	172 ± 17	150 ± 12	0.87	<0.0039[c]
No. of sperm/ cauda (10^6)	7.70 ± 3.45	3.30 ± 0.81	0.43	<0.0007[c]

[a] Mice from the C57BL/6J background were used at 8 weeks of age.
[b] Twelve mice of each genotype were used.
[c] Values were statistically significant (Student's *t* test).

4.6% of tubules with at least one vacuole) (Fig. 2D); such vacuoles were rarely present in aged wild-type testes. Interestingly, the weights of testes from 8-week-old *Taf7l*$^{-/Y}$ mice were 10% less than those of wild-type males (*P* < 0.0039). The sperm counts of *Taf7l*$^{-/Y}$ mice were reduced by >50% (*P* < 0.0007) (Table 1).

in *Taf7l*$^{-/Y}$ testes (Fig. 2C). In contrast, the abundance of TAF7 is not affected in *Taf7l*$^{-/Y}$ testes.

Expression of TFIID components in *Taf7l*$^{-/Y}$ testes. Two independent nuclear extracts made from wild-type or mutant testes were analyzed for the expression of TFIID components (Fig. 3). Our results showed that no significant change in expression of TBP or the other TAFs (TAF5 and TAF6) was observed in *Taf7l*$^{-/Y}$ testes (Fig. 3A). Nuclear extracts were immunoprecipitated with antibodies against TBP. As expected, TAF7L was coimmunoprecipitated with TBP from wild-type but not *Taf7l*$^{-/Y}$ testes (Fig. 3B). As previously described, little TAF7 was precipitated with TBP in the wild type, whereas a significantly larger amount was found in the immunoprecipitated fraction from *Taf7l*$^{-/Y}$ testes (Fig. 3B) (30). These results suggest that there is competition between TAF7 and TAF7L for integration into TFIID so that in the presence of TAF7L, TAF7 is excluded, whereas in its absence, TAF7 can more readily associate with TBP. However, TAF7 did not appear to be upregulated in *Taf7l*-deficient spermatids (see Fig. S1 in the supplemental material).

Reduced sperm production and fertility in *Taf7l*$^{-/Y}$ mice. Both *Taf7l*$^{-/Y}$ males and *Taf7l*$^{-/-}$ females appeared to be grossly healthy and produced healthy offspring. However, we found that although *Taf7l*$^{-/Y}$ males were fertile, they produced smaller litters. The litter size (average ± standard deviation) sired by *Taf7l*$^{-/Y}$ males (3.8 ± 2.1) was sharply reduced in comparison to that of wild-type littermate controls (8.3 ± 2.5) (*P* < 0.0004). The body weight of *Taf7l*$^{-/Y}$ males was similar to that of wild-type littermates. Histological analysis of 8-week-old *Taf7l*$^{-/Y}$ testes revealed no spermatogenic arrest, as evidenced by the presence of a full range of spermatogenic cells, including spermatogonia, spermatocytes, and spermatids (data not shown). However, aged *Taf7l*$^{-/Y}$ testes (>7 months old) developed large vacuoles in seminiferous tubules (15.2% ±
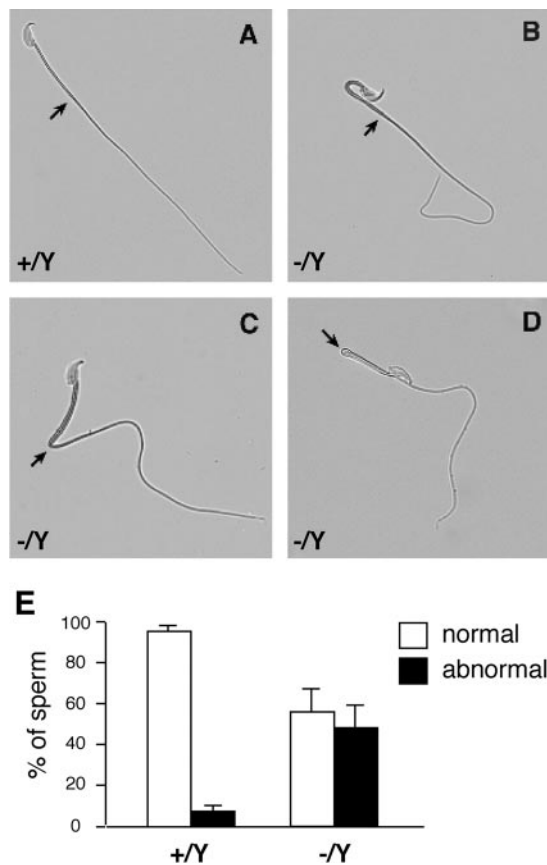

FIG. 4. Morphological defects in *Taf7l*-deficient sperm. Sperm from adult cauda epididymides were analyzed. (A) Wild-type sperm. (B) *Taf7l* mutant sperm folded at the proximal middle piece. The sperm head is bent back on the tail. (C) Flagellar angulation of *Taf7l* mutant sperm at the distal middle piece. (D) The middle piece is bent over the principal piece. In addition, the principal piece of *Taf7l* mutant sperm is abnormally curved. Arrows indicate a junction between the middle and principal pieces. (E) Percentage of sperm with normal and angulated tails. Three 8-week-old mice of each genotype (*Taf7l*$^{+/Y}$ or *Taf7l*$^{-/Y}$) were analyzed. Two hundred sperm from cauda epididymides were counted for each animal.
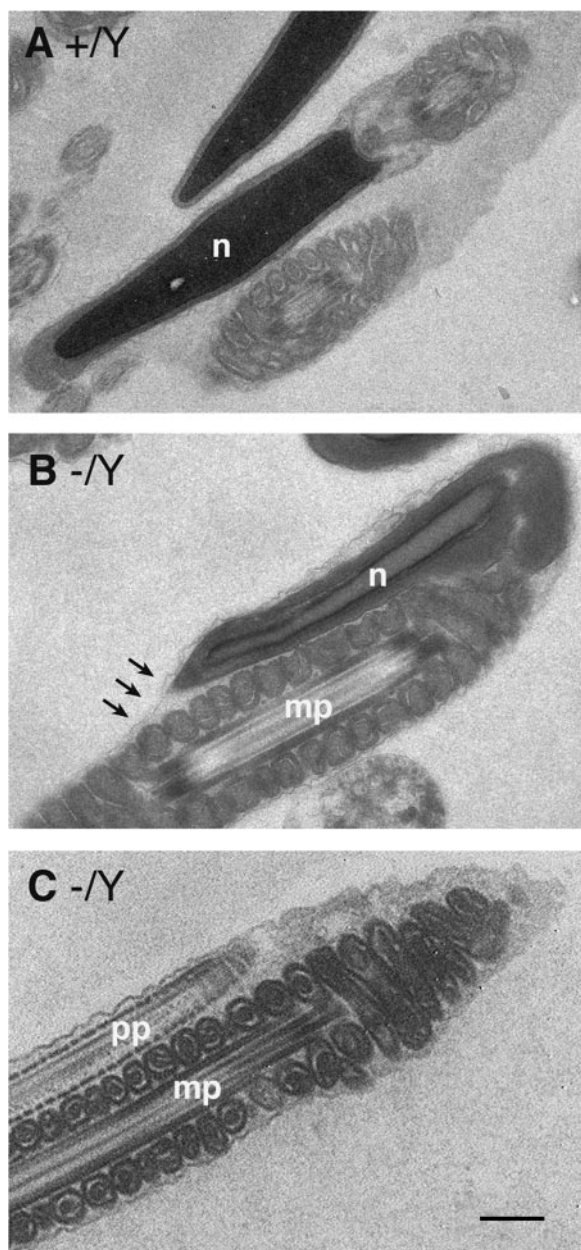
FIG. 5. Ultrastructural defects in *Taf7l*-deficient sperm. (A) Wild-type sperm. (B) *Taf7l* mutant sperm. The sperm head (n) is folded over the middle piece (mp). Arrows indicate the continuity of the cytoplasmic membrane from the apex of the sperm head to the middle piece. (C) *Taf7l* mutant sperm. The principal piece (pp) is bent 180° over the middle piece around the annulus. Bar, 500 nm.

Structural defects and impaired motility in sperm from *Taf7l*$^{-/Y}$ mice. During the sperm count analysis, we observed that a high percentage of sperm tails from *Taf7l*$^{-/Y}$ mice were folded (Fig. 4). Sperm tails were frequently bent by 180° within the middle piece (Fig. 4B) or at the junction between the middle and principal pieces (Fig. 4D). Sharp angulation of sperm tails also occurred at the junction of the middle and principal pieces (Fig. 4C). Overall, 46% of *Taf7l*$^{-/Y}$ sperm tails were folded or angulated, compared with 5.8% in the wild type (Fig. 4E).

We further examined the sperm tail defects by electron microscopy (Fig. 5). When the sperm head was folded back on the middle piece, the cytoplasmic membrane appeared to be retracted from the region of folding and thus extended continuously from the apex of the sperm head onto the middle piece (Fig. 5B). We confirmed that a high percentage of sperm tails folded around the annulus (the junction of the middle and principal pieces) (Fig. 5C).

We analyzed sperm motility by computer-assisted sperm analysis under both noncapacitating and capacitating conditions. The percentage of motile sperm was significantly reduced in *Taf7l*$^{-/Y}$ mice in comparison with that in the wild type (Table 2). Consistently, the values of three velocity parameters (VAP, VSL, and VCL) were significantly lower for *Taf7l*$^{-/Y}$ mice. However, the BCF of *Taf7l* mutant sperm was significantly higher, which is consistent with the observation that sperm with folded tails beat more rapidly but fail to generate forward motion. Surprisingly, the motility of mutant sperm was further reduced from 56.3% to 45.5% upon capacitation (Table 2).

Altered gene expression in *Taf7l*$^{-/Y}$ testes. To identify genes with altered expression in *Taf7l*$^{-/Y}$ testes systematically, we performed transcript profiling of testes from 8-week-old mice using Affymetrix Mouse Genome 430 2.0 GeneChips, representing more than 39,000 transcripts. With an expression cutoff of twofold change or greater, our microarray analysis identified 16 genes that were downregulated in *Taf7l*$^{-/Y}$ testes. Quantitative PCR analysis validated the downregulation of six genes (out of 16) in *Taf7l*$^{-/Y}$ testes, including four genes with known functions or motifs (*Cpa6*, 2.7-fold; *Adc*, 2.4-fold; *Sfmbt2*, 2.3-fold; and *Fscn1*, 3.4-fold) and two genes of unknown function (Table 3). CPA6 and ADC are metabolic enzymes. SFMBT2 (sex comb-like with four mbt domains 2) is a PcG protein and thus a putative transcription factor. Interestingly, FSCN1 is a widely expressed actin-bundling protein involved in cell motility (1). FSCN3, a testis-specific paralogue of FSCN1, localizes specifically to the elongating

TABLE 2. Motility of sperm from *Taf7l*$^{+/Y}$ and *Taf7l*$^{-/Y}$ mice[a]

Genotype and condition	Motility (%)	VAP (μm/s)	VSL (μm/s)	VCL (μm/s)	ALH (μm)	BCF (Hz)	STR (%)	LIN (%)
+/Y								
Uncapacitated	72.7 ± 4.2	166.9 ± 13.0	123.9 ± 11.4	270.6 ± 28.1	12.3 ± 0.8	10.5 ± 1.5	73.3 ± 1.5	47.3 ± 3.1
Capacitated	70.0 ± 15.6	160.3 ± 13.1	121.5 ± 9.2	261.0 ± 34.6	12.8 ± 3.2	15.0 ± 8.1	73.5 ± 2.1	48.0 ± 2.8
−/Y								
Uncapacitated	56.3 ± 2.1*	93.8 ± 5.1*	66.3 ± 3.5*	161.6 ± 14.6*	9.4 ± 1.4	19.6 ± 0.8*	69.3 ± 6.0	43.3 ± 5.0
Capacitated	45.5 ± 9.2*	90.0 ± 23.3*	63.3 ± 13.8*	154.3 ± 39.2*	9.3 ± 1.8	20.5 ± 2.5*	69.0 ± 4.2	45.5 ± 9.2

[a] Values represent means ± standard deviations. Three mice of each genotype were analyzed. Asterisks indicate statistically significant differences ($P < 0.05$). ALH, amplitude of lateral head displacement; STR, straightness; LIN, linearity.

TABLE 3. Downregulation of six genes in $Taf7l^{-/Y}$ testes

Gene symbol	Accession no.	Description	Fold decrease	
			Microarray	Real-time PCR
Fscn1	NM_007984	Fascin homolog 1, actin-bundling protein	4.6	3.4
4732473B16Rik	BB407092	RIKEN cDNA 4732473B16 gene	2.4	3.3
Cpa6	NM_177834	Carboxypeptidase A6	2.1	2.7
Adc	AV282351	Arginine decarboxylase	2.2	2.4
D1Ertd622e	NM_133825	DNA segment, chromosome 1, ERATO Doi 622, expressed	2.1	2.3
Sfmbt2	BM200222	Scm-like with four mbt domains 2	2.7	2.3

spermatid head (34). However, the expression of *Fscn3* is not altered in $Taf7l^{-/Y}$ testes, as assayed by both microarray and quantitative PCR analyses.

We then examined the expression of these six genes during spermatogenesis (Table 3). Even though they were all expressed in spermatids, the expression profiles of these genes during spermatogenesis were quite diverse (Fig. 6). Interestingly, *Cpa6* was specifically expressed in round spermatids. The expression level of *Adc* was relatively low in spermatogonia and early spermatocytes but increased in pachytene spermatocytes and peaked in round spermatids. The transcript level of *4732473B16Rik* was highest in early spermatocytes. *Fscn1*, *Sfmbt2*, and *D1Ertd622e* appeared to be expressed throughout spermatogenesis. We then asked whether these genes are germ cell specific by examining their expression in wild-type and germ cell-deficient (XX^{Y*}) testes (21). This analysis showed that two genes (*4732473B16Rik* and *Cpa6*) were germ cell specific, three genes (*Fscn1*, *Adc*, and *D1Ertd622e*) were expressed in germ cells at a higher level than in somatic cells of testes, and *Sfmbt2* was expressed at similar levels between germ cells and somatic cells in the testis (Fig. 6).

DISCUSSION

Although *Taf7l* is testis specific, it appears to be the ancestral gene from which *Taf7* originated by retroposition. A number of known retrogenes are derived from generally expressed X-linked ancestral genes, and most of these retrogenes are testis specific (22, 38). Therefore, the evolution of *Taf7* as a retrogene is an exception in that it is widely expressed. One possibility is that *Taf7l* was initially widely expressed (as the ancestral housekeeping gene). When *Taf7* was produced by retroposition during evolution and was widely expressed in somatic tissues, *Taf7l* evolved to be specialized in the testis with no selection pressure from the soma. This explanation is further supported by the presence of only one *Taf7* homologue in the chicken (*Gallus gallus*) genome. The chicken *Taf7* gene, comprising 11 introns, is present on the region of chromosome 4 that is syntenic with the *Taf7l*-containing region of the mammalian X chromosome, indicating that the chicken *Taf7* gene is orthologous to the mammalian *Taf7l* gene. Strikingly, the only other two X-linked TAF genes (*TAF1* and *TAF9B*) in mammals both have autosomal homologues (*TAF1L* and *TAF9*) (15, 40). Interestingly, the *TAF1L* gene is testis specific, arose by retroposition relatively recently in the old-world monkey lineage, including humans, and can functionally substitute the

somatic TAF1 (40). These studies point to the unique selection pressure on X-linked TAFs and the continuous creation of testis-specific TAFs during evolution.

Recent studies support the notion that special transcription mechanisms operate in germ cells (23, 33). Apart from the presence of testis-specific TAFs, TRF2/TLF is a testis-specific paralogue of TBP. Disruption of *Trf2* in mice causes spermiogenic arrest and thus male sterility (28, 44). In comparison, the loss of TAF7L results in reduced fertility but not sterility. Although TAF7L is missing from TFIID, only a small number of genes are affected. The relatively mild phenotypes caused by the loss of TAF7L are surprising. However, the enhanced reproductive fitness (increased sperm count, increased sperm motility, and increased litter size) conferred by *Taf7l* in one generation has probably had dramatic cumulative effects on an evolutionary time scale.

The transcript levels of six genes are reduced in $Taf7l^{-/Y}$ testis more than twofold. The deficiency of *Taf7l* might be compensated in part but not fully by *Taf7*, suggesting that *Taf7l* has evolved specialized functions in transcription regulation in spermatogenesis. It is possible that developmental stage-specific transcripts might be missed by the microarray profiling of
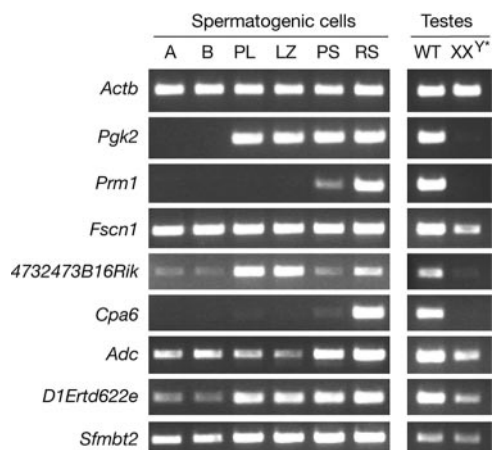

FIG. 6. Expression analysis during spermatogenesis. Relative transcript levels among different spermatogenic cell populations were assayed by RT-PCR. *Actb* served as a ubiquitous expression control. *Pgk2* is transcribed at the onset of meiosis. *Prm1* is expressed in postmeiotic germ cells. A, type A spermatogonia; B, type B spermatogonia; PL, preleptotene spermatocytes; LZ, mixed leptotene and zygotene spermatocytes; PS, pachytene spermatocytes; RS, round spermatids; WT, wild-type adult testes; XX^{Y*}, germ cell-deficient adult testes.

whole testes. However, the altered transcript levels of these six genes might be implicated in the sperm defects (amount, morphology, and motility) in $Taf7l^{-/Y}$ mice. The most strongly downregulated gene is $Fscn1$ (Table 3). FSCN1 is a filamentous actin (F actin)-bundling protein involved in cytoplasmic protrusion and cell motility (1). In mammalian spermatozoa, actin filaments are found primarily in the subacrosomal space along the nucleus (37). The actin cytoskeleton undergoes dynamic changes in sperm capacitation and the acrosome reaction (5). Globular actin polymerizes to form F actin during capacitation. Prior to the acrosome reaction, F actin undergoes depolymerization. Actin is also detected in the outer dense fibers of the sperm tail, suggesting that actin may regulate sperm motility (3, 13, 29). We postulate that altered expression of $Fscn1$ contributes to reduced sperm motility and folding of sperm tails in $Taf7l^{-/Y}$ testes. In addition, mutant sperm motility is further reduced upon capacitation (Table 2). These results suggest that bundling of F actin is important for the regulation of sperm motility and capacitation. However, the mechanism underlying FSCN1 function in spermatozoa remains to be determined. In addition, the expression of two metabolic enzymes (CPA6 and ADC) in spermatids might also be related to sperm function (Fig. 6).

In *Drosophila*, testis-specific TAFs oppose transcriptional repression mediated by PcG proteins, and both groups of proteins localize to the nucleolus in spermatocytes (8). Interestingly, $Sfmbt2$ encodes a PcG protein of unknown function and is downregulated in $Taf7l^{-/Y}$ testes. In addition to nuclear localization in pachytene spermatocytes and round spermatids, TAF7L localizes to specific chromatin domains in meiotically dividing spermatocytes (30). These results suggest that cross talk between testis-specific TAFs and PcG proteins in the regulation of gene-selective transcription in male germ cell differentiation might be conserved between *Drosophila* species and mice.

Here, we show that targeted disruption of $Taf7l$ in mice results in reduced sperm count and motility. $Taf7l$ is an X-linked, single-copy testis-specific gene in both mice and humans (39). Thus, the human $TAF7L$ gene may also play an important role in spermatogenesis. Because of the hemizygous state of the X chromosome in men, mutations in $TAF7L$ might cause oligozoospermia (reduced sperm count) in humans.

REFERENCES

1. **Adams, J. C.** 2004. Roles of fascin in cell adhesion and motility. Curr. Opin. Cell Biol. **16:**590–596.

2. **Albright, S. R., and R. Tjian.** 2000. TAFs revisited: more data reveal new twists and confirm old ideas. Gene **242:**1–13.

3. **Aumüller, G., and J. Seitz.** 1988. Immunocytochemical localization of actin and tubulin in rat testis and spermatozoa. Histochemistry **89:**261–267.

4. **Bell, B., E. Scheer, and L. Tora.** 2001. Identification of hTAF(II)80 delta links apoptotic signaling pathways to transcription factor TFIID function. Mol. Cell **8:**591–600.

5. **Breitbart, H., G. Cohen, and S. Rubinstein.** 2005. Role of actin cytoskeleton in mammalian sperm capacitation and the acrosome reaction. Reproduction **129:**263–268.

6. **Brou, C., S. Chaudhary, I. Davidson, Y. Lutz, J. Wu, J. M. Egly, L. Tora, and P. Chambon.** 1993. Distinct TFIID complexes mediate the effect of different transcriptional activators. EMBO J. **12:**489–499.

7. **Camacho, J. A., N. Rioseco-Camacho, D. Andrade, J. Porter, and J. Kong.** 2003. Cloning and characterization of human ORNT2: a second mitochondrial ornithine transporter that can rescue a defective ORNT1 in patients with the hyperornithinemia-hyperammonemia-homocitrullinuria syndrome, a urea cycle disorder. Mol. Genet. Metab. **79:**257–271.

8. **Chen, X., M. Hiller, Y. Sancak, and M. T. Fuller.** 2005. Tissue-specific TAFs counteract Polycomb to turn on terminal differentiation. Science **310:**869–872.

9. **Chiang, C. M., and R. G. Roeder.** 1995. Cloning of an intrinsic human TFIID subunit that interacts with multiple transcriptional activators. Science **267:**531–536.

10. **Dubrovskaya, V., A. C. Lavigne, I. Davidson, J. Acker, A. Staub, and L. Tora.** 1996. Distinct domains of hTAFII100 are required for functional interaction with transcription factor TFIIF beta (RAP30) and incorporation into the TFIID complex. EMBO J. **15:**3702–3712.

11. **Eggan, K., H. Akutsu, J. Loring, L. Jackson-Grusby, M. Klemm, W. M. Rideout III, R. Yanagimachi, and R. Jaenisch.** 2001. Hybrid vigor, fetal overgrowth, and viability of mice derived by nuclear cloning and tetraploid embryo complementation. Proc. Natl. Acad. Sci. USA **98:**6209–6214.

12. **Falender, A. E., R. N. Freiman, K. G. Geles, K. C. Lo, K. Hwang, D. J. Lamb, P. L. Morris, R. Tjian, and J. S. Richards.** 2005. Maintenance of spermatogenesis requires TAF4b, a gonad-specific subunit of TFIID. Genes Dev. **19:**794–803.

13. **Fouquet, J. P., M. L. Kann, and J. P. Dadoune.** 1990. Immunoelectron microscopic distribution of actin in hamster spermatids and epididymal, capacitated and acrosome-reacted spermatozoa. Tissue Cell **22:**291–300.

14. **Freiman, R. N., S. R. Albright, S. Zheng, W. C. Sha, R. E. Hammer, and R. Tjian.** 2001. Requirement of tissue-selective TBP-associated factor TAFII105 in ovarian development. Science **293:**2084–2087.

15. **Frontini, M., E. Soutoglou, M. Argentini, C. Bole-Feysot, B. Jost, E. Scheer, and L. Tora.** 2005. TAF9b (formerly TAF9L) is a bona fide TAF that has unique and overlapping roles with TAF9. Mol. Cell. Biol. **25:**4638–4649.

16. **Gegonne, A., J. D. Weissman, and D. S. Singer.** 2001. TAFII55 binding to TAFII250 inhibits its acetyltransferase activity. Proc. Natl. Acad. Sci. USA **98:**12432–12437.

17. **Green, M. R.** 2000. TBP-associated factors (TAFIIs): multiple, selective transcriptional mediators in common complexes. Trends Biochem. Sci. **25:**59–63.

18. **Hiller, M., X. Chen, M. J. Pringle, M. Suchorolski, Y. Sancak, S. Viswanathan, B. Bolival, T. Y. Lin, S. Marino, and M. T. Fuller.** 2004. Testis-specific TAF homologs collaborate to control a tissue-specific transcription program. Development **131:**5297–5308.

19. **Hiller, M. A., T. Y. Lin, C. Wood, and M. T. Fuller.** 2001. Developmental regulation of transcription by a tissue-specific TAF homolog. Genes Dev. **15:**1021–1030.

20. **Hochheimer, A., and R. Tjian.** 2003. Diversified transcription initiation complexes expand promoter selectivity and tissue-specific gene expression. Genes Dev. **17:**1309–1320.

21. **Hunt, P. A., and E. M. Eicher.** 1991. Fertile male mice with three sex chromosomes: evidence that infertility in XYY male mice is an effect of two Y chromosomes. Chromosoma **100:**293–299.

22. **Khil, P. P., B. Oliver, and R. D. Camerini-Otero.** 2005. X for intersection: retrotransposition both on and off the X chromosome is more frequent. Trends Genet. **21:**3–7.

23. **Kimmins, S., N. Kotaja, I. Davidson, and P. Sassone-Corsi.** 2004. Testis-specific transcription mechanisms promoting male germ-cell differentiation. Reproduction **128:**5–12.

24. **Lavigne, A. C., G. Mengus, M. May, V. Dubrovskaya, L. Tora, P. Chambon, and I. Davidson.** 1996. Multiple interactions between hTAFII55 and other TFIID subunits. Requirements for the formation of stable ternary complexes between hTAFII55 and the TATA-binding protein. J. Biol. Chem. **271:**19774–19780.

25. **Lee, M. A., and B. T. Storey.** 1986. Bicarbonate is essential for fertilization of mouse eggs: mouse sperm require it to undergo the acrosome reaction. Biol. Reprod. **34:**349–356.

26. **Lewandoski, M., E. N. Meyers, and G. R. Martin.** 1997. Analysis of Fgf8 gene function in vertebrate development. Cold Spring Harbor Symp. Quant. Biol. **62:**159–168.

27. **Lin, T. Y., S. Viswanathan, C. Wood, P. G. Wilson, N. Wolf, and M. T. Fuller.**

1996. Coordinate developmental control of the meiotic cell cycle and spermatid differentiation in Drosophila males. Development **122:**1331–1341.

28. **Martianov, I., G. M. Fimia, A. Dierich, M. Parvinen, P. Sassone-Corsi, and I. Davidson.** 2001. Late arrest of spermiogenesis and germ cell apoptosis in mice lacking the TBP-like TLF/TRF2 gene. Mol. Cell **7:**509–515.

29. **Paranko, J., A. Yagi, and M. Kuusisto.** 1994. Immunocytochemical detection of actin and 53 kDa polypeptide in the epididymal spermatozoa of rat and mouse. Anat. Rec. **240:**516–527.

30. **Pointud, J. C., G. Mengus, S. Brancorsini, L. Monaco, M. Parvinen, P. Sassone-Corsi, and I. Davidson.** 2003. The intracellular localisation of TAF7L, a paralogue of transcription factor TFIID subunit TAF7, is developmentally regulated during male germ-cell differentiation. J. Cell Sci. **116:**1847–1858.

31. **Roeder, R. G.** 1996. The role of general initiation factors in transcription by RNA polymerase II. Trends Biochem. Sci. **21:**327–335.

32. **Russell, L. D., R. A. Ettlin, A. P. Sinha Hikim, and E. D. Clegg.** 1990. Histological and histopathological evaluation of the testis. Cache River Press, Clearwater, FL.

33. **Sassone-Corsi, P.** 2002. Unique chromatin remodeling and transcriptional regulation in spermatogenesis. Science **296:**2176–2178.

34. **Tubb, B., D. J. Mulholland, W. Vogl, Z. J. Lan, C. Niederberger, A. Cooney, and J. Bryan.** 2002. Testis fascin (FSCN3): a novel paralog of the actin-bundling protein fascin expressed specifically in the elongate spermatid head. Exp. Cell Res. **275:**92–109.

35. **Veenstra, G. J., and A. P. Wolffe.** 2001. Gene-selective developmental roles of general transcription factors. Trends Biochem. Sci. **26:**665–671.

36. **Verrijzer, C. P., and R. Tjian.** 1996. TAFs mediate transcriptional activation and promoter selectivity. Trends Biochem. Sci. **21:**338–342.

37. **Vogl, A. W., K. Genereux, and D. C. Pfeiffer.** 1993. Filamentous actin detected in rat spermatozoa. Tissue Cell **25:**33–48.

38. **Wang, P. J.** 2004. X chromosomes, retrogenes and their role in male reproduction. Trends Endocrinol. Metab. **15:**79–83.

39. **Wang, P. J., J. R. McCarrey, F. Yang, and D. C. Page.** 2001. An abundance of X-linked genes expressed in spermatogonia. Nat. Genet. **27:**422–426.

40. **Wang, P. J., and D. C. Page.** 2002. Functional substitution for TAFII250 by a retroposed homolog that is expressed in human spermatogenesis. Hum. Mol. Genet. **11:**2341–2346.

41. **Wang, P. J., D. C. Page, and J. R. McCarrey.** 2005. Differential expression of sex-linked and autosomal germ-cell-specific genes during spermatogenesis in the mouse. Hum. Mol. Genet. **14:**2911–2918.

42. **Yang, F., R. Fuente De La, N. A. Leu, C. Baumann, K. J. McLaughlin, and P. J. Wang.** 2006. Mouse SYCP2 is required for synaptonemal complex assembly and chromosomal synapsis during male meiosis. J. Cell Biol. **173:**497–507.

43. **Yang, F., H. Skaletsky, and P. J. Wang.** 2007. *Ubl4b*, an X-derived retrogene, is specifically expressed in post-meiotic germ cells in mammals. Gene Expr. Patterns **7:**131–136.

44. **Zhang, D., T. L. Penttila, P. L. Morris, M. Teichmann, and R. G. Roeder.** 2001. Spermiogenesis deficiency in mice lacking the *Trf2* gene. Science **292:**1153–1155.

45. **Zhou, T., and C. M. Chiang.** 2001. The intronless and TATA-less human TAF(II)55 gene contains a functional initiator and a downstream promoter element. J. Biol. Chem. **276:**25503–25511.